

Evaluating the effect of wind-driven patchiness on trophic interactions between zooplankton and phytoplankton

E. A. Blukacz,^{a,1} W. G. Sprules,^{a,*} B. J. Shuter,^{b,c} and J. P. Richards^d

^aDepartment of Biology, University of Toronto, Mississauga, Ontario, Canada

^bDepartment of Ecology and Evolutionary Biology, University of Toronto, Toronto, Ontario, Canada

^cHarkness Laboratory of Fisheries Research, Ontario Ministry of Natural Resources, Peterborough, Ontario, Canada

^dFaculty of Information, University of Toronto, Toronto, Ontario, Canada

Abstract

We measured spatial patterns of zooplankton and chlorophyll concentration (a proxy for phytoplankton) with continuous sensors along horizontal transects that were repeatedly sampled ($n = 150$) under varying wind conditions throughout a growing season in two basins (South Arm and Annie Bay) of Lake Opeongo, Ontario, Canada. Spatially explicit in situ simulations that included activity costs associated with feeding were used to examine the effects of chlorophyll patchiness on the energy gain in different zooplankton communities. Simulations were repeated for several zooplankton size classes (small, large, and bulk) and two communities (all copepods and all cladocerans). For each simulated combination, a spatial energetic differential (SED) was estimated by contrasting the energy that zooplankton could gain using observed spatial patterns in chlorophyll and water temperature with the energy they could gain using uniform concentrations of chlorophyll and water temperature. Large zooplankton showed the greatest SED range across all communities, from a decrease of 8% to a maximum increase of 20%, assuming relatively low costs associated with feeding activity. Small zooplankton had the narrowest SED range. Zooplankton energy gain is sensitive to both the degree of zooplankton–chlorophyll spatial overlap and energetic costs associated with zooplankton feeding activity. SED values as high as 485% can occur under plausible estimates of activity costs. Wind-driven increases in spatial overlap between predator and prey can be large enough to substantially alter planktonic trophic interactions.

In marine and freshwater ecosystems, both phytoplankton and zooplankton have patchy distributions that occur over a wide range of spatiotemporal scales. Although there is general agreement that the predominant drivers of spatial heterogeneity in phytoplankton distributions are physical (e.g., wind-driven currents), the relative importance of physical vs. biological drivers for zooplankton spatial distributions has been the subject of more debate (Martin 2003). Recent work is shifting this view by demonstrating that physical drivers, by themselves, are insufficient to explain the observed spatial structure across all scales (Martin 2003). The “multiple driving forces hypothesis” (Pinel-Alloul 1995) contends that physical drivers have strong control of zooplankton patchiness at large scales, but that the strength of biological drivers increases at small scales.

Zooplankton play an important role in trophic interactions as they prey on phytoplankton and serve as food for fish. To gain a better understanding of such interactions, many researchers have used computer simulations (Martin 2003). Most simulations to date have estimated predator (zooplankton) consumption using statistical distributions, rather than observed data, to generate the predator patchiness, the prey (phytoplankton) patchiness, or both (Martin 2003). A few studies have computed consumption directly from observed data (Mullin and Brooks 1976;

Sprules 2000). Mullin and Brooks (1976) conducted their study on a single predator species using a relatively coarse spatial scale, and although Sprules (2000) used data from a wider range of spatial scales, his consumption calculations were still limited to a single species. None of the studies above demonstrated a link between wind-driven or biologically driven patchiness and trophic interactions. Recently, Blukacz et al. (2009) documented details of the spatial patterns of zooplankton and phytoplankton associated with wind-driven water movement. They showed that large-scale (> 1 km) downwind accumulation of zooplankton and phytoplankton was positively correlated with wind force, whereas small-scale (< 1 km) patterns depended on the speed and persistence of the wind. In this companion study, we evaluate how these in situ wind-driven spatial patterns may affect spatially explicit simulations of zooplankton energy potential. Our focus will be on the horizontal patterns of spatial overlap between predator (zooplankton) and prey (phytoplankton) observed by Blukacz et al. (2009) at a fixed depth (~ 2 m) during the day. These observations are largely free of the immediate effects of diurnal vertical migration and hence we will not consider this process in our analyses.

Blukacz et al. (2009) also showed that spatial patterns of zooplankton varied with body size as well as wind exposure. Copepods select larger food particles than cladocerans, and studies have shown that grazing rates can be relatively higher when cladocerans are dominant (Peters and Downing 1984; Cyr 1998). We therefore contrast simulations of large- and small-bodied zooplankton and of communities comprising only copepods or only cladocerans to address these grazing effects.

* Corresponding author: gary.sprules@utoronto.ca

¹Current address: Environment Canada, 4905 Dufferin St., Toronto, Ontario, Canada

The zooplankton literature does not provide a complete empirical assessment of the activity costs associated with feeding (Lampert 1988; Svetlichny and Hubareva 2005). As a result, activity costs are not incorporated into most studies of zooplankton feeding and bioenergetics. This is in marked contrast to the decades of attention paid by fish ecologists to the role that activity costs play in shaping the bioenergetics of individuals (Boisclair and Leggett 1989; Rennie et al. 2005) and the character of populations (Sherwood et al. 2002b; Kaufman et al. 2009). We have used the literature on fish activity costs as a guide to including activity costs in our assessment of how the joint spatial distribution of predator and prey determines zooplankton feeding efficiency. There are several studies in the zooplankton literature that provide a sound basis for a simple activity cost model: (1) zooplankton respiration rates have been shown to increase with swimming speed (Steele and Mullin 1977; Buskey 1998; Swadling et al. 2005) and the costs of swimming alone can be significant: for example, Swadling et al. (2005) measured the respiration rate of starved *Euphausia superba* under minimal (standard metabolic rate) and maximal activity levels and showed that swimming costs could account for up to 73% of the total daily respiration rate; (2) cladocerans and copepods reduce swimming speed when they enter food patches and remain in the patches by performing area-restricted search behavior (Leising and Franks 2002); (3) the mechanical costs of filtering for copepods (Kjørboe et al. 1985) and cladocerans (Lampert 1986) are negligible; (4) increases in respiration rates during feeding are due primarily to biochemical digestion costs (specific dynamic action [SDA] in the fisheries bioenergetics literature; Kitchell et al. 1977). Combining all of these observations, we arrive at an activity model in which costs of swimming vary inversely with food concentration whereas costs of digestion vary directly with consumption. We will use this model to explore the influence of activity costs on net energy gain by zooplankton in all of our simulations.

In this paper, we use field-measured spatial distributions of zooplankton, chlorophyll, and water temperatures, collected under widely varying wind conditions, as a template upon which we superimpose our activity model to explore the effects of spatial patterning on the bioenergetics of zooplankton. We contrast the potential energy gain achievable by zooplankton, under observed spatial distributions, with the potential gain achievable under uniform spatial distributions with mean values identical to observed means. Our hypothesis is that the kinds of spatial distributions observed in the field will yield higher energy gains for zooplankton than those expected from uniform spatial distributions.

Methods

Field collections—To determine the effect of wind exposure on trophic interactions, we collected zooplankton, phytoplankton, and water temperature data in Lake Opeongo over a wide range of scales during windy and calm conditions. Lake Opeongo, located in central Ontario within Algonquin Park (45°42'N, 78°22'W) is oligotrophic

(total phosphorus ranged from 6 to 8 mg m⁻³) and comprises four basins, two of which were sampled. Annie Bay, the smaller basin, has a long axis of 4.2 km oriented perpendicularly to prevailing northwesterly winds, a surface area of 4.4 km², and a maximum depth of 24 m. South Arm has a long axis of 5.8 km oriented parallel to prevailing winds, a surface area of 22.1 km², and a maximum depth of 50 m. A linear transect in each basin (~ 3 km long in Annie Bay, ~ 4.8 km in South Arm) was sampled 75 times during the day between mid-July and mid-September 2001 and 2003 (fig. 1 in Blukacz et al. 2009). Transects were sampled with continuously recording sensors that measured zooplankton abundance and body size (optical plankton counter [OPC]), chlorophyll concentration (fluorometer), water temperature (conductivity–temperature–depth probe [CTD]), and water volume (digital flowmeter). The sensors were towed through the epilimnion at a constant depth of 2.5 m and recorded the total number of animals (OPC) or an average value (CTD and fluorometer) every 1.5 linear m or a volume of roughly 3 liters. Further details of the sampling protocol are outlined by Blukacz et al. (2009).

Organisms passing through the OPC block light in proportion to their size and orientation, and this triggers a voltage pulse that is calibrated to the diameter of a sphere (equivalent spherical diameter [ESD]). The fresh mass (μg) of each animal was determined assuming a specific gravity of 1 and using the volume of an oblate spheroid with major axis = ESD (Blukacz et al. 2009). Studies on zooplankton from Canadian lakes have used several zooplankton size classes (Masson et al. 2004) and these represent mainly micro- and macrozooplankton. We divided zooplankton into the five size classes that were approximately equally abundant across all our samples: < 355 μm , 355–399 μm , 399–451 μm , 451–542 μm , and > 542 μm ESD. Although all size classes were analyzed, we focused on the results from the smallest (355–399 μm) and largest (> 542 μm) classes to clearly illustrate how particle size affects the range of wind-driven trophic interactions. We also reported results for bulk zooplankton samples (all size categories combined, < 355 μm to > 542 μm). Analyses were performed using the biomass ($\mu\text{g L}^{-1}$) of zooplankton in our three size classes, the concentration of chlorophyll ($\mu\text{g L}^{-1}$), and the water temperature ($^{\circ}\text{C}$). Hereafter, the zooplankton biomass size classes are referred to simply as bulk, small, or large. The OPC is limited to recording zooplankton that have an ESD > 250 μm , so some rotifers and small copepod nauplii were not recorded (Sprules et al. 1998). In Lake Opeongo, the OPC recorded 90% of the zooplankton biomass where the biomass was dominated by copepods followed by cladocerans.

Zooplankton energetic potential—We used computer simulations to evaluate the effect that observed spatial patterns have on the energetic potential (i.e., the net energy gain) of zooplankton communities using in situ data collected over a wide range of wind conditions. Each sampling transect ($n = 150$) served as an independent observation for the simulations and consisted of a measure of zooplankton biomass in the three size classes and a

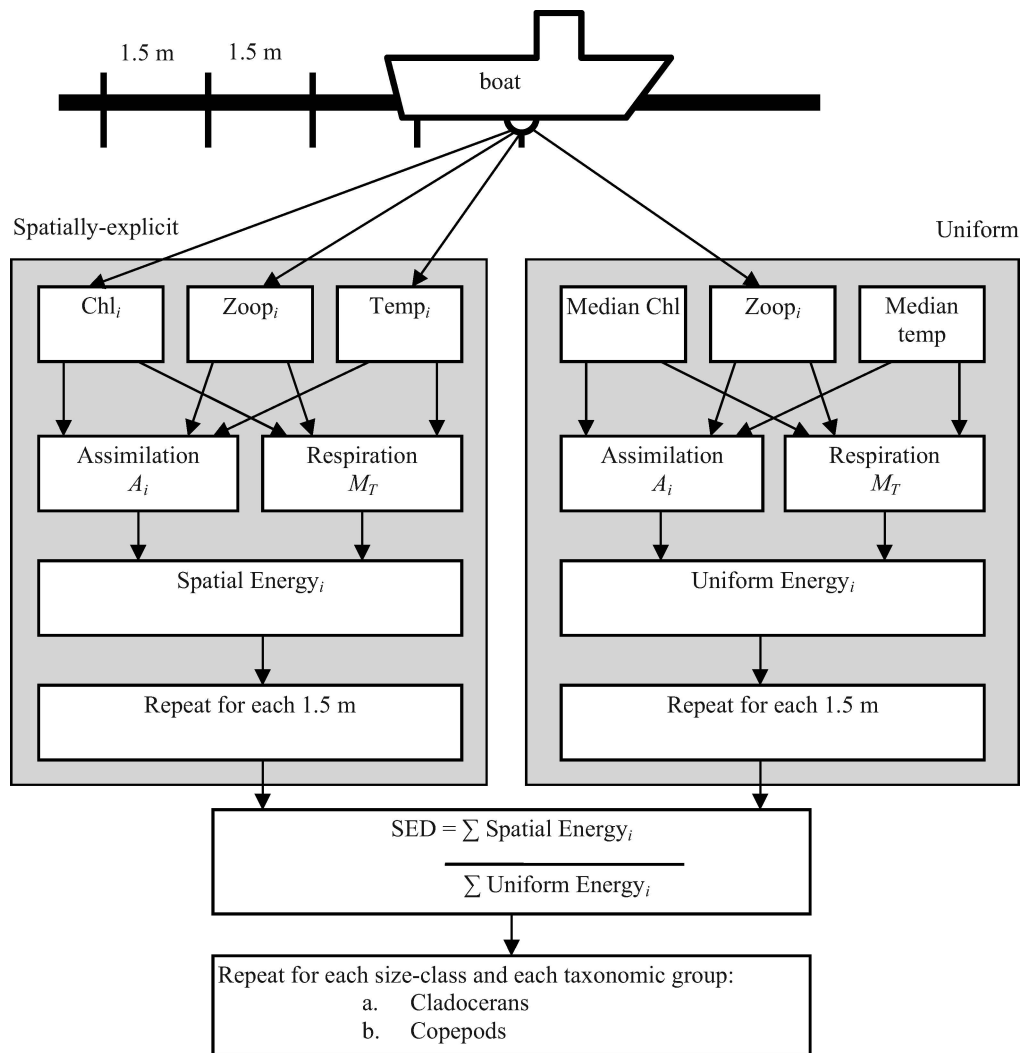


Fig. 1. A flowchart of the simulation steps involved in the SED simulations. Chl_i , $Temp_i$, and $Zoop_i$ represent a measurement of each variable in the i th sampling unit. The difference between assimilation (A) and total metabolism (= respiration; M_T) is the energy potential for each of the i sampling units that is used to estimate $SpatialEnergy_i$ and $UniformEnergy_i$.

measurement each of water temperature and chlorophyll concentration for every 1.5 m (Fig. 1). For each transect, zooplankton energy potential was calculated using the observed spatial patterns and contrasted with uniform conditions in which each 1.5 m was characterized by the transect median value of temperature and chlorophyll concentration. The energy potential was estimated as the difference between assimilation (the amount of food absorbed by the gut) and respiration (Lampert 1986). All processes were expressed in units of carbon ($\mu\text{g C animal}^{-1} \text{d}^{-1}$). Assimilation was estimated as a proportion (0.70) of consumption rate (Downing and Rigler 1984), hence assuming egestion of about 30%. We recognize that assimilation rates can vary depending on factors such as food quality and quantity (Straile 1997), but our goal in this paper was to focus on the effects of spatial patterns on the potential energy gain by zooplankton, not on how variability in assimilation rate might modify that gain.

Zooplankton consumption and respiration rates were predicted from statistical models. To date, the multiple regression model of Peters and Downing (1984) provides the most comprehensive review of freshwater and marine zooplankton consumption rates and environmental conditions. We used their data and fit reduced models of consumption rates (Y) for freshwater copepods and cladocerans with animal weight (W), food concentration (S), and water temperature (T) as predictors:

$$\log(Y) = a + b \log(W) + c \log(S) + d(\log S)^2 + gT + hT^2 \quad (1)$$

Predictors that remained significant ($\alpha = 0.05$) after Bonferroni correction were retained. The simplest models that explained the most variability were chosen (*see* Table 1 for final models). In these calculations, we used a dry : fresh mass ratio for zooplankton of 0.2, a specific gravity = 1, a chlorophyll : volume ratio of 0.003363, and a carbon : wet mass ratio for algae of 0.1.

Table 1. The models used to predict consumption for the two taxon-specific communities (cladoceran and copepod) where Y is the consumption rate ($\mu\text{g C animal}^{-1} \text{d}^{-1}$), W is dry animal weight (μg), S is food concentration (mg L^{-1}), and T is water temperature ($^{\circ}\text{C}$). For each model, the p values, the partial correlations, and the p values for each predictor are indicated.

Community	Model	p value and R^2	Partial correlations		
			$\text{Log}(W)$	$\text{Log}(S)$	T
Cladocerans	$\text{Log}(Y) = 0.447 + 0.639\text{Log}(W) + 0.495\text{Log}(S)$	$p < 0.001$ 0.590	$p < 0.05$ 0.279	$p < 0.05$ 0.233	
Copepods	$\text{Log}(Y) = -0.055745 + 0.537\text{Log}(W) + 0.748\text{Log}(S) - 0.153\text{Log}(S^2) + 0.045T + 0.024$	$p < 0.001$ 0.326	$p < 0.05$ 0.180	$p < 0.05$ 0.190	$p < 0.05$ 0.049

We modeled respiration using Steele and Mullin's (1977) definition of total metabolism (M_T):

$$M_T = M_1 + M_2 + M_3 \quad (2)$$

where M_1 is standard metabolic rate and M_2 and M_3 are the respiratory costs of digestion and activity, respectively. We predicted standard metabolic rate (M_1) from body weight (W) and water temperature (T) using Ikeda et al.'s (2001) model:

$$\ln(M_1) = -0.399 + 0.801(W) + 0.069(T) \quad (3)$$

In this calculation, we used a dry: fresh mass and a carbon: dry mass ratio for zooplankton of 0.1 and 0.5363 respectively, and a respiratory quotient of 0.83. The respiration cost associated with the biochemical costs of digesting food (M_2) was proportional to assimilation rate (A) and SDA, the respiratory costs associated with food digestion:

$$M_2 = \text{SDA} \times A \quad (4)$$

The SDA coefficient was set at 0.15 (Lampert 1986).

Activity costs—Although Steele and Mullin (1977) included swimming costs (M_3), they did not provide a method of calculating them. We combined published studies to estimate M_3 by assuming it has a negative linear relationship with chlorophyll concentration (Fig. 2). This is appropriate because others have reported a linear increase in respiration rates with swimming speed (Buskey 1998; Swadling et al. 2005) and that zooplankton movement slows within food patches (Jensen et al. 2001). We define limits of M_3 for two conditions: at zero chlorophyll concentration and at the average incipient limiting concentration, the point at which maximum consumption rates are reached and swimming is no longer required for prey capture. At zero chlorophyll concentration zooplankton swim as they search for prey, but not as quickly as they did in the artificially forced swimming experiments that are typically used to measure maximal respiration rates (Lampert 1984). We therefore used half the standard metabolic cost ($M_3 = 0.5 \times M_1$), a value that falls within the low to mid range of measured maximal swimming-related values of 0.2 to 5 times standard metabolism (Torres and Childress 1983; Morris et al. 1990; Buskey 1998). The incipient limiting chlorophyll concentration ($8.5 \mu\text{g L}^{-1}$) was calculated from table 5 in Chow-Fraser

and Sprules (1992). At this food concentration, swimming is assumed to cease and $M_3 = 0$. The final equation used to predict M_3 was

$$M_3 = 0.5M_1 \times \frac{(8.5 - S)}{8.5} \quad (5)$$

for $S < 8.5$ and $M_3 = 0$ for $S \geq 8.5$, where S is the chlorophyll concentration ($\mu\text{g L}^{-1}$).

Simulation scenarios—Simulations were performed for each zooplankton size class (bulk, small, and large), using separate consumption equations for copepods and cladocerans (Table 1) to represent different communities. For each 1.5 m record along a transect, a spatial energy value (SpatialEnergy_i) was calculated for each individual zooplankton as the difference between assimilation and respiration. A uniform energy value (UniformEnergy_i) was also computed using the median chlorophyll concentration and water temperature for the entire transect. The spatial energetic differential (SED) was estimated for each transect by dividing the sum of the all of the individual spatial energy values by the sum of all of the individual uniform energy values:

$$\text{SED} = \frac{\sum \text{SpatialEnergy}_i}{\sum \text{UniformEnergy}_i} \quad (6)$$

SEDs range from greater than 1 through 1 to less than 1, indicating an energetic advantage in spatially explicit distributions, no energetic advantage, and an energetic disadvantage, respectively.

Predator-prey spatial overlap—In both basins, for each transect, multi-scale wavelet correlations were performed to determine the degree of spatial overlap between zooplankton biomass (all size classes) and chlorophyll concentration for eight different scales ($\lambda_1 \dots \lambda_8$): 3–6, 6–12, 12–24, 24–48, 48–96, 96–192, 192–384, and 384–768 m. Hereafter, these are referred to as wavelet correlations. The advantage over traditional methods is that wavelet correlations are computed on a scale-by-scale basis (Gençay et al. 2002).

The maximal overlap discrete wavelet transform with the Daubechies filter (least asymmetric filter LA8) was used to decompose the input data into the eight spatial scales. The LA8 filter was used because it is better at conserving the variability at a given scale than the commonly used Haar filter (Gençay et al. 2002; Blukacz et al. 2009). The decomposition yields two sets of wavelet coefficients for each scale, one for a zooplankton size class (X) and the

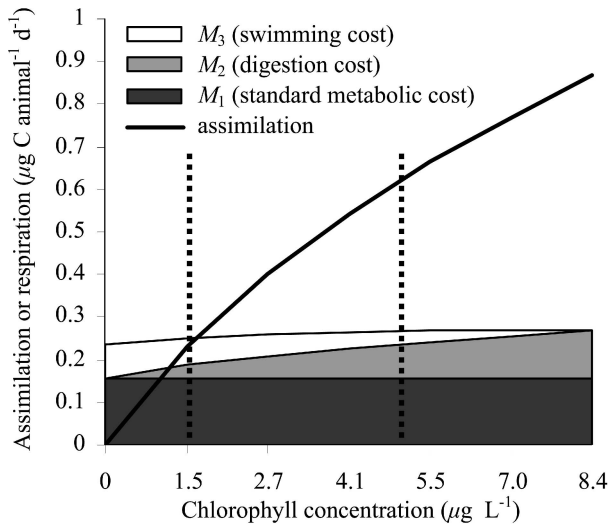


Fig. 2. Assimilation and total metabolism as a function of chlorophyll concentration. Total metabolism is the sum of basal metabolism (M_1), digestion (M_2), and activity (M_3) for a 12- μg animal. Assimilation is 0.7 times consumption rate (see Table 1) using the copepod model. The range of chlorophyll concentration for Lake Opeongo is between 1.5 and 5.0 $\mu\text{g L}^{-1}$ as indicated by the dashed vertical lines.

other for the chlorophyll concentration (Y):

$$\tilde{W}_X(\lambda_j) = (W_1 \dots W_{\tilde{N}}) \text{ and } \tilde{W}_Y(\lambda_j) = (W_1 \dots W_{\tilde{N}}) \quad (7)$$

For each scale, the covariance ($\bar{c}_j = \tilde{\gamma}(\lambda_j)$) between the two sets of wavelet coefficients was computed as the sum of their products divided by the number of coefficients unaffected by boundary conditions (\tilde{N}):

$$\bar{c}_j = \tilde{\gamma}(\lambda_j) = \frac{\sum \tilde{W}_{Xj} \times \tilde{W}_{Yj}}{\tilde{N}_j} \quad (8)$$

(Gençay et al. 2002). Wavelet variances were computed for each variable:

$$\bar{a}_j = \hat{\sigma}_X^2(\lambda_j) \text{ and } \bar{b}_j = \hat{\sigma}_Y^2(\lambda_j) \quad (9)$$

and these were used to compute wavelet correlation coefficient for each scale as

$$\tilde{\rho}(\lambda_j) = \frac{\bar{c}_j}{\sqrt{\bar{a}_j \times \bar{b}_j}} \quad (10)$$

(Gençay et al. 2002). The significance of wavelet correlations for each scale was assessed by confidence intervals (CIs). The upper and lower CIs were computed with $\alpha = 0.05$, assuming a normal distribution:

$$\text{CIs}(\lambda_j) = \tanh \left\{ \tilde{\rho}(\lambda_j) \pm \xi_{\frac{\alpha}{2}} \left(\frac{1}{\tilde{N}_j - 3} \right)^{1/2} \right\} \quad (11)$$

where $\xi_{\alpha/2}$ is a quantile from a normal distribution and \tanh is Fisher's z -transformation for nonlinearity, which maps the CIs back to a range between -1 and 1 (Gençay et al. 2002). After the correlations were performed, the percent-

age of transects with significant positive and negative correlations ($\alpha = 0.05$) was determined for each scale, in both basins.

Results

Zooplankton energetic potential—Partial correlations in our consumption models showed that animal weight and chlorophyll concentration explained most of the variation for cladocerans and copepods respectively (Table 1). In South Arm, large zooplankton had the highest SEDs (up to a 9% increase), and small zooplankton had the lowest increase across all communities (Fig. 3A,B). In Annie Bay, SEDs were more variable across all simulations (Fig. 3C,D). Large zooplankton also had the highest SEDs, reaching a maximum increase of 20%, whereas small zooplankton had the narrowest range. The median SEDs were all slightly greater than 1 in both basins, regardless of simulation scenario, indicating that inclusion of spatial patterns resulted in an energetic advantage. Some SEDs were less than 1, indicating that inclusion of spatial patterns can result in an energetic disadvantage.

In both basins, large copepods had the most frequent energy advantage, especially in animals in South Arm, with an energy advantage occurring up to 82% of the time (Table 2). In contrast, small copepods in both basins had the lowest percentage of transects with an energy advantage and the highest percentage of transects with an energy disadvantage. Cladocerans in both basins showed on average a 14% lower energy advantage than copepods across all size classes.

Predator-prey spatial overlap—Multi-scale wavelet correlations quantified the degree of spatial overlap between zooplankton biomass (all size classes) and chlorophyll concentration in both basins. Only significant ($\alpha = 0.05$) correlations (positive and negative) were reported. Generally, if more than one correlation was reported for a given transect, then all of them were either positive or negative. In South Arm, the percentage of positive associations between chlorophyll concentration and zooplankton biomass increased with spatial scale, peaking at 192–384 m for all size classes, except for the small zooplankton that tended to be negatively associated with chlorophyll (Fig. 4A,C). By contrast, in Annie Bay there were very few strong associations between zooplankton and chlorophyll concentration, with slightly more positive associations (Fig. 4B,D).

In each basin, to determine if predator-prey spatial overlap (positive wavelet correlations) led to an energetic advantage (SED greater than 1), the percentages of positive and negative correlations across all spatial scales were calculated for three SED categories (less than 1, equal to zero, and greater than 1). These calculations were repeated for each simulation scenario. As an example, for copepods the simulation for large zooplankters showed that 53% of transects in the South Arm had both significant positive correlations and SED values greater than 1. However, as the percentage of positive correlations decreased, so too did the energetic advantage, indicating that predator-prey spatial overlap is an important determinant of SED

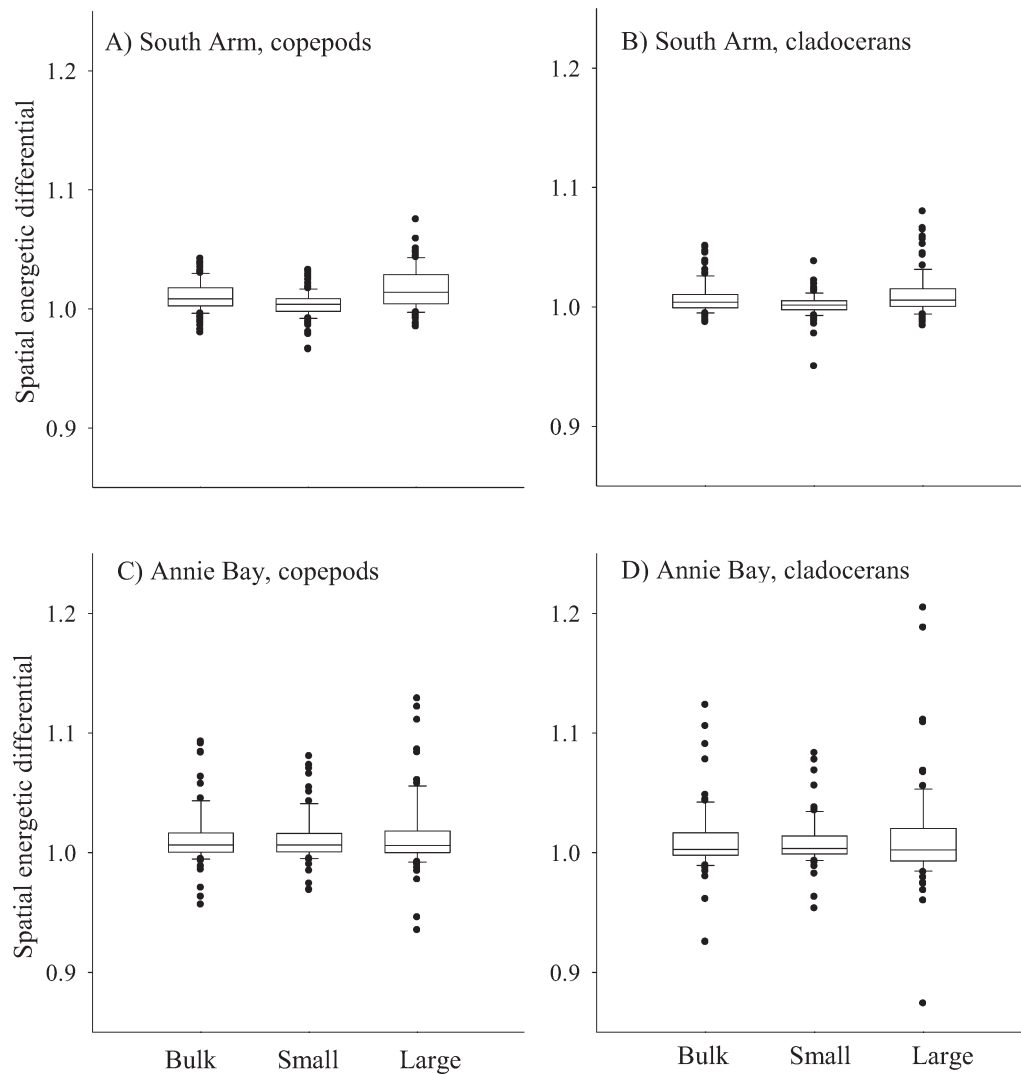


Fig. 3. Output from simulations of SEDs for (A, B) the South Arm and (C, D) Annie Bay. Zooplankton size classes are labeled as bulk, small, and large, and the zooplankton communities are also labeled as either only copepods or only cladocerans. The interquartile range is represented by the boxes with medians marked by horizontal lines, the whiskers represent first and third quartiles, and values outside the whiskers are extremes.

(Fig. 5A,B). A similar pattern was observed for large zooplankton in Annie Bay (Fig. 5C,D). In contrast, small zooplankton did not show a clear pattern of correlations with chlorophyll among the three SED categories in either basin (Fig. 5A,C).

Discussion

Detailed zooplankton energy budget calculations are typically performed in a laboratory with a focus on a single species. Only a few studies have used in situ zooplankton

Table 2. The percentage of transects for each simulation scenario that fell into the three SED categories: (1) greater than 1 (> 1.005), indicating an energetic advantage; (2) equal to 1 (≥ 0.995 and ≤ 1.005), indicating no advantage; and (3) less than 1 (< 0.995), indicating a disadvantage. Copepods and cladocerans refer to communities consisting entirely of these organisms.

Basin	Spatial energetic differential	Copepods			Cladocerans		
		Bulk	Small	Large	Bulk	Small	Large
South Arm	>1	77.14	57.14	81.90	60.95	45.71	68.57
	$=1$	17.14	33.33	13.33	32.38	45.71	24.76
	<1	5.71	9.52	4.76	6.67	8.57	6.67
Annie Bay	>1	65.75	61.64	67.12	50.68	50.27	60.27
	$=1$	27.40	30.14	26.03	38.36	26.03	31.51
	<1	6.85	8.22	6.85	10.96	23.29	8.22

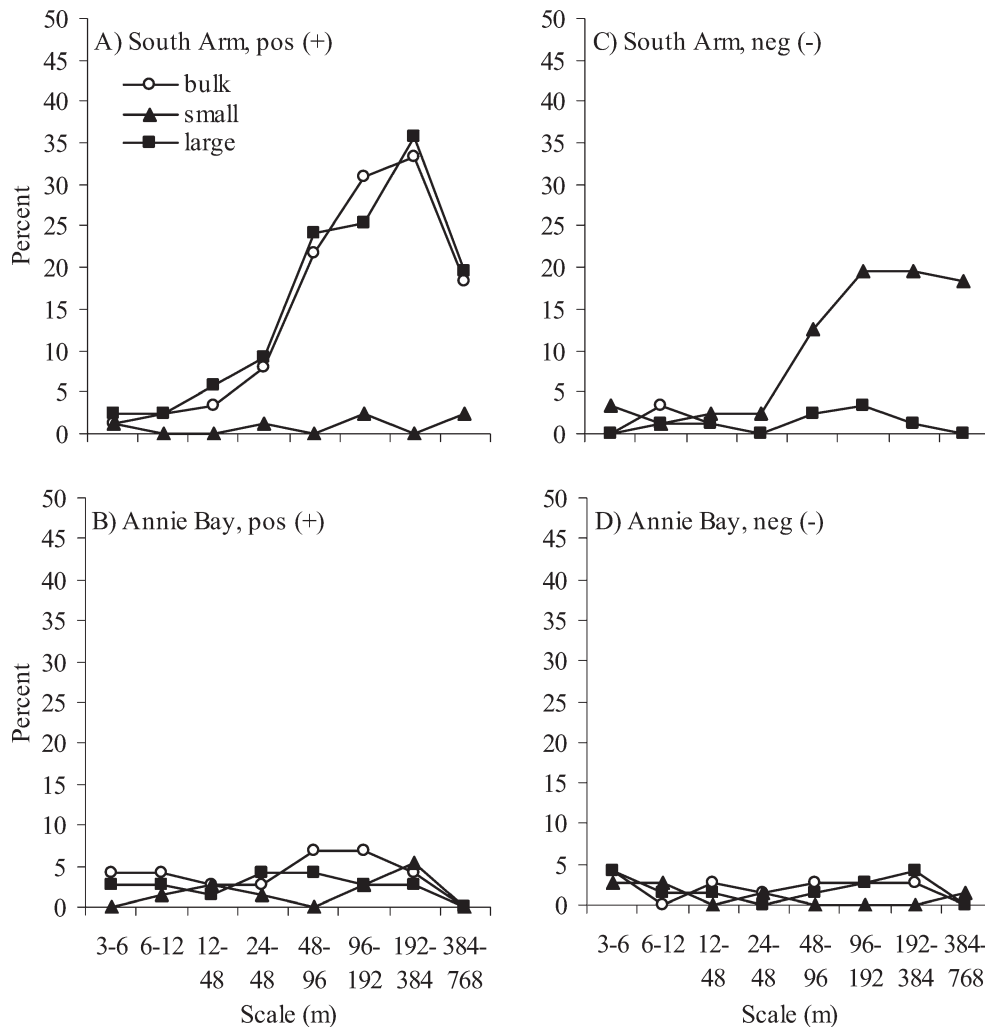


Fig. 4. Percentage of sampling transects with significant positive (pos +) and negative (neg -) wavelet correlations between zooplankton and chlorophyll concentration for eight spatial scales in (A, C) the South Arm and (B, D) Annie Bay.

data (Mullin and Brooks 1976; Sprules 2000) collected at different spatial scales to examine trophic consequences. However, unlike the community-based budgets here, Mullin and Brooks' (1976) budgets were restricted to a single species sampled only twice at 10 fixed stations. They concluded that an energetic disadvantage occurred 50% of the time, but recognized that their results were limited because turbulent water movement may constantly rearrange predator-prey spatial patterns. Sprules (2000) used OPC data collected over a wide range of spatial scales and computed consumption rates for two separate sampling events, and concluded that consumption rates differed by fourfold between two separate sampling events, but he did not measure wind conditions. Recently, Blukacz et al. (2009) demonstrated that in Lake Opeongo, water temperature (proxy for water movement) and zooplankton and phytoplankton spatial patterns are mainly driven by wind. They showed that large-scale (> 1 km) downwind accumulation increased with wind force and small-scale

(< 1 km) variability of spatial patterns increased with wind speed. These spatial patterns occurred more frequently in South Arm, which had a larger fetch than Annie Bay, resulting in greater wind exposure (Blukacz et al. 2009). Furthermore, they show that patterns, at both scales (downwind accumulation and increased variability), occurred more frequently during windy conditions. In this companion study, we used simulations to evaluate the effect that observed spatial patterns have on the SED for all combinations of two types of zooplankton communities (only copepods and only cladocerans) and three zooplankton size classes (bulk, small, and large). Across all of the simulation scenarios, these budgets predicted that including the observed spatial patterns can result in an energetic advantage in up to 82% of the transects sampled (Table 2). Data were recorded every 1.5 m, resulting in at least 1600 records per transect, which provided relatively high-resolution snapshots of predator-prey interactions. In addition, 150 transects were sampled over a wide range of

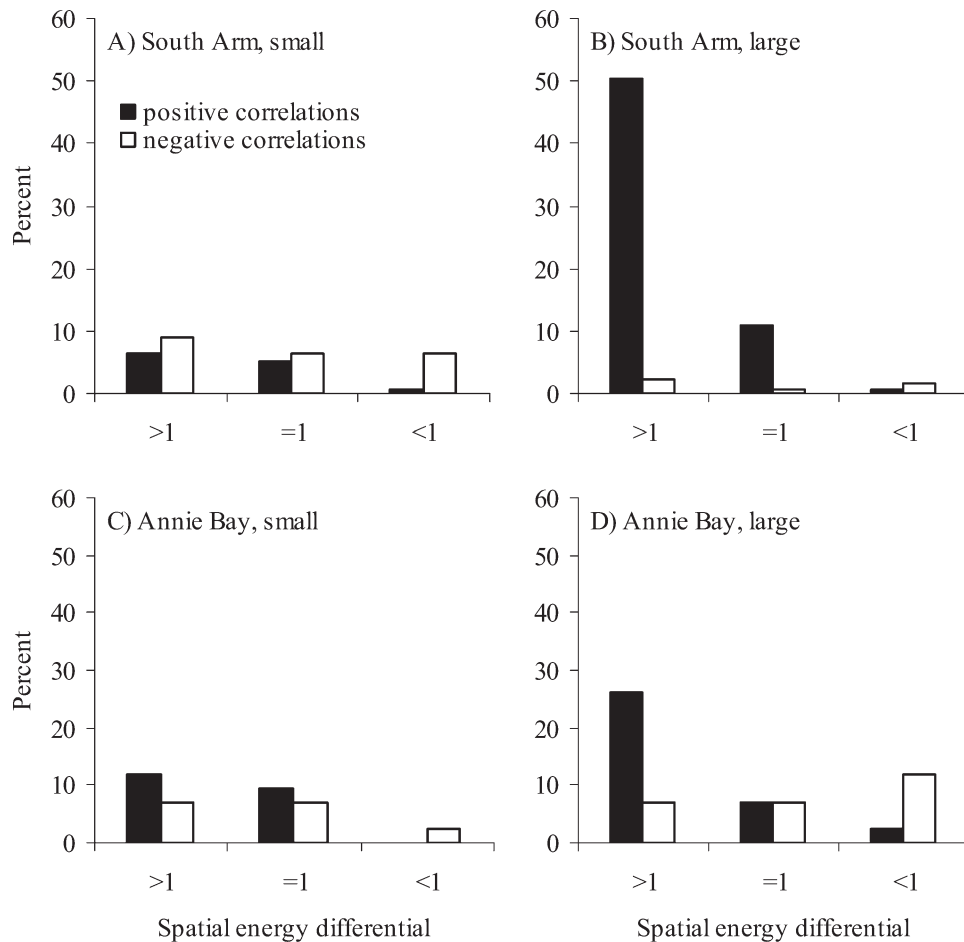


Fig. 5. The percent of significant positive (black bars) and negative (open bars) wavelet correlations (summed across scales) between chlorophyll concentration and (A, C) small zooplankton and (B, D) large zooplankton are shown for both basins.

wind conditions, resulting in high replication, which ensured that these interactions were captured as the relative strength of wind conditions changed.

Across basins and communities, large zooplankton were predicted to have the highest SEDs and small zooplankton the lowest energy advantage (Fig. 3). This is a reflection of size-specific differences in consumption rates because body weight was an important predictor of consumption (Table 1). On average, small zooplankton were predicted to have consumption rates that were approximately 2.5 times lower than those of large animals. Although respiration rates also increase with body size, the energy gain for larger zooplankton was estimated to be approximately 1.8 times higher than that for small animals at the same food concentration.

We used chlorophyll as a proxy for phytoplankton because the upper layers of each basin were well mixed, with relatively consistent species composition among replicate samples from each basin. However, South Arm had a greater potential of large-scale patterns (downwind accumulation) because 58% of the seasonal average phytoplankton biomass consisted of motile species (mainly dinoflagellates, average size 23 μm long by 33 μm wide) that tend to float, compared to 19% in Annie Bay, whereas

cyanobacteria accounted for less than 1% of biomass (Blukacz et al. 2009). The spatial patterns of chlorophyll were the main driver of consumption rates and these, in turn, were the main determinants of SED. Wavelet correlations showed that transects with SEDs greater than 1 also showed the most positive correlations between predator and prey, especially for the large size class (Fig. 5). Negative associations also existed, but these were more frequent in transects that had SEDs less than 1. Wind-driven water movement is likely generating the degree of predator-prey overlap observed in our samples. Studies have shown that both zooplankton and phytoplankton aggregate downwind at large scales (> 1 km), whereas at smaller scales Langmuir circulation may also foster spatial overlap (George 1981; Wetzel 2001; Blukacz et al. 2009). At smaller scales (a few meters) zooplankton can actively swim and adjust their spatial overlap with their food, if the current speeds do not exceed their swimming speeds (Stich and Lampert 1981). In this study, it is unlikely that even the largest zooplankters, such as *Daphnia*, which can move 0.08 cm s^{-1} , were able to control their horizontal position at the sampled depth (2.5 m), because the observed currents exceed 1 cm s^{-1} even at the slowest wind speeds (Stich and Lampert 1981). However, zooplankton may still

be able to control their vertical position by moving lower in the water column because currents show an exponential decay with depth (Kalf 2002). This was not the case for the small zooplankton that tended to be randomly distributed (H. Cyr pers. comm.).

Previous studies have documented zooplankton–phytoplankton interactions through correlation analysis, but the trophic consequences of such interactions were not quantified (Mackas and Boyd 1979; Star and Mullin 1981; Malone and McQueen 1983). Studies have also shown that zooplankton spatial patterns can differ depending on body size (Martin and Srokosz 2002), especially if these patterns are wind-driven (Blukacz et al. 2009). Our simulations clearly illustrated that zooplankton trophic interactions are size-specific, because large zooplankton were predicted to have the highest energetic advantage. We recommend that future studies take these size-specific differences into consideration when sampling and modeling zooplankton communities. In addition, new technologies such as the FluoroProbe can be used to obtain more precise data on spatial variation in prey availability by distinguishing between edible and inedible phytoplankton.

Clearly, predators benefit from a strong spatial overlap with high food concentrations. In reality, a predator would be exposed to a wide range of food concentrations as the relative strengths of biological and physical drivers change. Current speeds were never measured in behavioral studies, but there is consistent evidence that copepods and cladocerans, when given a choice of food concentrations, find and remain in food patches (Cuddington and McCauley 1994; Larsson 1997; Jensen et al. 2001). Similarly, studies have also found that swimming activity decreases in larval fish as food concentration increases (Sirois and Boisclair 1995). Our study is the first attempt to include digestive and swimming costs associated with area-restricted search behavior in energy budget calculations. Swadlow et al. (2005) showed that swimming costs of starved animals can range from 13% to 73% of their total daily respiration rates, but digestion costs were not included in their assessment as all experiments were performed on starved animals. Most zooplankton studies measure respiration rates on starved animals and report activity costs as a multiplier of standard metabolism (Lampert 1984). We used 1.5 times the standard metabolic rate predicted by Ikeda et al.'s (2001) model, which falls in the lower to mid range of published values (Torres and Childress 1983; Morris et al. 1990; Buskey 1998). Activity costs have been included in fish energy budgets for many years (Kitchell et al. 1977), with a cost ~ 2 times standard metabolic rate commonly assumed. Recently, new methods have been developed to measure fish activity costs directly in the field. These included contaminant–bioenergetic mass balance approaches (Rennie et al. 2005), direct observations (Boisclair and Leggett 1989) and enzyme indicator approaches (e.g., the use of lactate dehydrogenase in Sherwood et al. 2002a,b). All of these studies consistently show that fish activity levels range from 1.5 to 5 times standard metabolic rate. Zooplankton activity costs also fall within this range, and so the maximal activity costs that we used were probably conservative considering that the

respiration rate predicted from Ikeda et al.'s (2001) equation falls somewhere between standard and routine metabolism. When we included activity costs of the order observed for fish by Rennie et al. (2005) in our simulations, SED values of 485% were predicted, indicating that our results may significantly underestimate the energetic advantage that wind-driven spatial overlap can provide to zooplankton and that a research focus on quantifying the magnitude of zooplankton activity costs in the wild is warranted.

In both basins, our simulations predicted that cladocerans tended to have a slightly narrower range in SEDs than copepods. Comparisons of SED differences showed that on average cladocerans had 34% less energy than copepods. This is a reflection of differences in consumption between copepods and cladocerans because respiration rates were estimated in the same manner for both communities. On average for the same food concentration, predicted copepod consumption rates were approximately 1.9 times the predicted cladoceran consumption rates. A closer examination of the Peters and Downing (1984) published consumption models also shows that copepod consumption rates were approximately 2.5-fold higher than cladoceran consumption rates. Studies have shown that when large cladocerans (> 1 mm body length), such as *Daphnia*, are highly abundant, they can consume large amounts of phytoplankton (Pace 1984). However, in Lake Opeongo large cladocerans only represented 6% of the total biomass (E.A.B. pers. obs.), and these types of communities are typical for low-productivity lakes such as Lake Opeongo (Cyr 1998). Cyr's (1998) in situ study of zooplankton communities showed that copepods have higher consumption rates on food particles greater than 35 μm in diameter. Cladocerans are generally filter feeders preferring smaller particles, whereas copepods graze less on smaller particles and generally prefer larger particles (Peters and Downing 1984; Horn 1985). In the current study, it was not possible to take particle size into account because the fluorometer records only chlorophyll concentration of the encountered algal particles. However, the consumption rates used here should reflect the studied communities because the reduced statistical models (Table 1) were validated using additional studies for both cladoceran and copepod species specific to Lake Opeongo.

This is the first study to use in situ data across a wide range of spatial scales and wind conditions to simulate energy budgets of different zooplankton communities. This study clearly illustrates that prey patchiness can be an important driver of zooplankton consumption rates as well as activity costs, whereas wind is an important driver of prey patchiness (Blukacz et al. 2009). There were distinct differences between the basins in SEDs, resulting from South Arm's being relatively more exposed to the prevailing winds than Annie Bay (Blukacz et al. 2009); this in turn led to an overall greater energy advantage for zooplankton living in South Arm because it increased the frequency of predator–prey spatial overlap (Figs. 4, 5). Therefore, explicit records of wind conditions should always be made when sampling over a wide range of spatial scales. Furthermore, running several transects over

a short period of time will not provide sufficient data to relate the observed spatial patterns to wind conditions and to determine the trophic consequences of such patterns simply because sudden changes in wind conditions may not be captured. Therefore, to best represent trophic interactions of zooplankton, spatial patterns along with wind conditions should be included in all calculations.

Acknowledgments

We are grateful to Charlie Menza, who gave us permission to use all of his 2001 data. We thank the staff of the Harkness Laboratory of Fisheries Research, Ontario Ministry of Natural Resources, for logistic support of fieldwork, and Mathew Blukacz for stepping in and helping out during a critical point in the summer of 2003. We are thankful for statistical discussions with Pierre Legendre and Marie-Josée Fortin, for discussions with Mathew Wells about the physics of water movement, and for discussions on modeling activity costs in zooplankton with Winfried Lampert. Thanks to Ikeda Tsutomu, Peder Yurista, and Edward Buskey for discussions on zooplankton metabolism, and to John Downing for providing zooplankton consumption data. George Arhonditsis provided very valuable comments that we applied in our simulations. Funding was provided through a Natural Sciences and Engineering Research Council of Canada Discovery Grant to W.G.S., the Great Lakes Fisheries Commission and the Ontario Ministry of Natural Resources to B.J.S., and University of Toronto scholarships to E.A.B. Comments on earlier versions of the manuscript by anonymous reviewers were very helpful.

References

- BLUKACZ, E. A., B. J. SHUTER, AND W. G. SPRULES. 2009. Towards understanding the relationship between wind conditions and plankton patchiness. *Limnol. Oceanogr.* **54**: 1530–1540.
- BOISCLAIR, D., AND W. C. LEGGETT. 1989. The importance of activity in bioenergetics models applied to actively foraging fish. *Can. J. Fish. Aquat. Sci.* **46**: 1859–1867, doi:10.1139/f89-234
- BUSKEY, E. J. 1998. Energetic costs of swarming behavior for the copepod *Dioithona oculata*. *Mar. Biol.* **130**: 425–431, doi:10.1007/s002270050263
- CHOW-FRASER, P., AND W. G. SPRULES. 1992. Type-3 functional-response in limnetic suspension-feeders, as demonstrated by *in situ* grazing rates. *Hydrobiologia* **232**: 175–191.
- CYR, H. 1998. Cladoceran- and copepod-dominated zooplankton communities graze at similar rates in low-productivity lakes. *Can. J. Fish. Aquat. Sci.* **55**: 414–422, doi:10.1139/cjfas-55-2-414
- CUDDINGTON, K. M., AND E. McCAULEY. 1994. Food-dependent aggregation and mobility of the water fleas *Ceriodaphnia dubia* and *Daphnia pulex*. *Can. J. Zool.* **72**: 1217–1226, doi:10.1139/z94-163
- DOWNING, J. A., AND F. H. RIGLER. 1984. A manual on methods for the assessment of secondary productivity in fresh waters. Blackwell Scientific.
- GENÇAY, R., F. SELÇUK, AND B. WHITCHER. 2002. An introduction to wavelets and other filtering methods in finance and economics. Academic.
- GEORGE, D. G. 1981. Wind-induced water movements in the south basin of Windermere. *Freshw. Biol.* **11**: 37–60, doi:10.1111/j.1365-2427.1981.tb01241.x
- HORN, W. 1985. Investigations into the food selectivity of the planktic crustaceans *Daphnia hyalina*, *Eudiaptomus gracilis* and *Cyclops vicinus*. *Int. Rev. Gesam. Hydrobiol.* **70**: 603–612, doi:10.1002/iroh.19850700412
- IKEDA, T., Y. KANNO, K. OZAKI, AND A. SHINADA. 2001. Metabolic rates of epipelagic marine copepods as a function of body mass and temperature. *Mar. Biol.* **139**: 587–596.
- JENSEN, K. H., P. LARSSON, AND G. HOGSTEDT. 2001. Detecting food search in *Daphnia* in the field. *Limnol. Oceanogr.* **46**: 1013–1020.
- KALFF, J. 2002. *Limnology*. Benjamin Cummings.
- KAUFMAN, S. D., G. E. MORGAN, AND J. M. GUNN. 2009. The role of ciscoes as prey in the trophy growth potential of walleyes. *N. Am. J. Fish. Manage.* **29**: 468–477, doi:10.1577/M07-117.1
- KJØRBOE, T., F. MOHLENBERG, AND H. U. RISSGARD. 1985. *In situ* feeding rates of planktonic copepods—a comparison of 4 methods. *J. Exp. Mar. Biol. Ecol.* **88**: 67–81, doi:10.1016/0022-0981(85)90202-3
- KITCHELL, J. F., D. J. STEWART, AND D. WEININGER. 1977. Applications of a bioenergetics model to yellow perch (*Perca flavescens*) and walleye (*Stizostedion vitreum vitreum*). *J. Fish. Res. Board Can.* **34**: 1922–1935.
- LAMPERT, W. 1984. The measurement of respiration, p. 413–468. *In* J. A. Downing and F. H. Rigler [eds.], *A manual on methods for the assessment of secondary production in fresh waters*. Blackwell Scientific.
- . 1986. Response of the respiratory rate of *Daphnia magna* to changing food conditions. *Oecologia* **70**: 495–501, doi:10.1007/BF00379894
- . 1988. The relationship between zooplankton biomass and grazing: A review. *Limnologia* **19**: 11–20.
- LARSSON, P. 1997. Ideal free distribution in *Daphnia*? Are daphnids able to consider both the food patch quality and the position of competitors? *Hydrobiologia* **360**: 143–152, doi:10.1023/A:1003128315850
- LEISING, A. W., AND P. J. S. FRANKS. 2002. Does *Acartia clausi* (Copepoda: Calanoida) use an area-restricted search foraging strategy to find food? *Hydrobiologia* **480**: 193–207, doi:10.1023/A:1021253622168
- MACKAS, D. L., AND C. M. BOYD. 1979. Spectral analysis of zooplankton heterogeneity. *Science* **204**: 62–64, doi:10.1126/science.204.4388.62
- MALONE, B. J., AND D. J. McQUEEN. 1983. Horizontal patchiness in zooplankton populations in two Ontario kettle lakes. *Hydrobiologia* **99**: 101–124, doi:10.1007/BF00015039
- MARTIN, A. P. 2003. Phytoplankton patchiness: The role of lateral stirring and mixing. *Prog. Oceanogr.* **57**: 125–174, doi:10.1016/S0079-6611(03)00085-5
- , AND M. A. SROKOSZ. 2002. Plankton distribution spectra: Inter-size class variability and the relative slopes for phytoplankton and zooplankton. *Geophys. Res. Lett.* **29**: 2213, doi:10.1029/2002GL015117
- MASSON, S., B. PINEL-ALLOUL, AND P. DUTILLEUL. 2004. Spatial heterogeneity of zooplankton biomass and size structure in southern Québec lakes: Variation among lakes and within lake among epi-, meta- and hypolimnion strata. *J. Plankton Res.* **26**: 1441–1458, doi:10.1093/plankt/fbh138
- MORRIS, M. J., K. KOHLAGE, AND G. GUST. 1990. Mechanics and energetics of swimming in the small copepod *Acanthocyclops robustus* (Cyclopoda). *Mar. Biol.* **107**: 83–91, doi:10.1007/BF01313245
- MULLIN, M. M., AND E. R. BROOKS. 1976. Some consequences of distributional heterogeneity of phytoplankton and zooplankton. *Limnol. Oceanogr.* **21**: 784–796, doi:10.4319/lo.1976.21.6.0784
- PACE, M. L. 1984. Zooplankton community structure, but not biomass, influences the phosphorous–chlorophyll *a* relationship. *Can. J. Fish. Aquat. Sci.* **41**: 1089–1096, doi:10.1139/f84-128

- PETERS, R. H., AND J. A. DOWNING. 1984. Empirical analysis of zooplankton filtering and feeding rates. *Limnol. Oceanogr.* **29**: 763–784, doi:10.4319/lo.1984.29.4.0763
- PINEL-ALLOUL, B. 1995. Spatial heterogeneity as a multiscale characteristic of zooplankton community. *Hydrobiologia* **301**: 17–42, doi:10.1007/BF00024445
- RENNIE, M. D., N. C. COLLINS, B. J. SHUTER, J. W. RAJOTTE, AND P. COUTURE. 2005. A comparison of methods for estimating activity costs of wild fish populations: More active fish observed to grow slower. *Can. J. Fish. Aquat. Sci.* **62**: 767–780, doi:10.1139/f05-052
- SHERWOOD, G. D., J. KOVACS, A. HONTELA, AND J. B. RASMUSSEN. 2002a. Simplified food webs lead to energetic bottlenecks in polluted lakes. *Can. J. Fish. Aquat. Sci.* **59**: 1–5, doi:10.1139/f01-213
- , I. PAZZIA, A. MOESER, A. HONTELA, AND J. B. RASMUSSEN. 2002b. Shifting gears: Enzymatic evidence for the energetic advantage of switching diet in wild-living fish. *Can. J. Fish. Aquat. Sci.* **59**: 229–241, doi:10.1139/f02-001
- SIROIS, P., AND D. BOISCLAIR. 1995. The influence of prey biomass on activity and consumption rates of brook trout. *J. Fish Biol.* **46**: 787–805, doi:10.1111/j.1095-8649.1995.tb01602.x
- SPRULES, W. G. 2000. Spatial estimates of prey consumption by *Mysis relicta* Loven using an optical plankton counter. *Int. Ver. Theor. Angew. Limnol. Verh.* **27**: 3275–3278.
- , J. D. STOCKWELL, AND A. W. HERMANN. 1988. Calibration of an optical plankton counter for use in fresh water. *Limnol. Oceanogr.* **43**: 726–733.
- STRAILE, D. 1997. Gross growth efficiencies of protozoan and metazoan zooplankton and their dependence on food concentration, predator-prey weight ratio, and taxonomic group. *Limnol. Oceanogr.* **42**: 1375–1385.
- STAR, J. L., AND M. M. MULLIN. 1981. Zooplankton assemblages in three areas of the North Pacific as revealed by continuous horizontal transects. *Deep-Sea Res.* **28**: 93–97.
- STEELE, J. H., AND M. M. MULLIN. 1977. Zooplankton dynamics, p. 857–890. *In* E. D. Goldberg [ed.], *The sea*. Wiley.
- STICH, H. B., AND W. LAMPERT. 1981. Predator evasion as an explanation of diurnal vertical migration by zooplankton. *Nature*. **293**: 396–400, doi:10.1038/293396a0
- SVETLICHNY, L. S., AND E. S. HUBAREVA. 2005. The energetics of *Calanus euxinus*: Locomotion, filtration of food and specific dynamic action. *J. Plankton Res.* **27**: 671–682, doi:10.1093/plankt/fbi041
- SWADLING, K. M., D. A. RITZ, S. NICOL, J. E. OSBORN, AND L. J. GURNEY. 2005. Respiration rate and cost of swimming for Antarctic krill, *Euphausia superba*, in large groups in the laboratory. *Mar. Biol.* **146**: 1169–1175, doi:10.1007/s00227-004-1519-z
- TORRES, J. J., AND J. J. CHILDRESS. 1983. Relationship of oxygen consumption to swimming speed in *Euphausia pacific*. 1. Effects of temperature and pressure. *Mar. Biol.* **74**: 79–86, doi:10.1007/BF00394278
- WETZEL, R. G. 2001. *Limnology*. Academic.

Associate editor: Christopher M. Finelli

Received: 31 August 2009

Accepted: 04 March 2010

Amended: 07 April 2010